Journal of Photochemistry and Photobiology A: Chemistry 223 (2011) 182–188

Contents lists available at SciVerse ScienceDirect

Journal of Photochemistry and Photobiology A: Chemistry

journal homepage: www.elsevier.com/locate/jphotochem

Water assisted photo-oxidation from hydroquinone to p-benzoquinone in a solid Ne matrix

Nobuyuki Akai*, Akio Kawai, Kazuhiko Shibuya*

Department of Chemistry, Graduate School of Science and Engineering, Tokyo Institute of Technology, 2-12-1-H57 Ohokayama, Meguro-ku, Tokyo 152-8551, Japan

ARTICLE INFO

Article history:
Received 4 February 2011
Received in revised form 3 August 2011
Accepted 19 August 2011
Available online 27 August 2011

Keywords:
Water complex
Photo-oxidation
Hydroquinone
Benzoquinone
Solid Ne matrix

ABSTRACT

Photochemistry of molecular complexes of hydroquinone (HQ) with water, HQ–$(water)_n$, were investigated by matrix-isolation FTIR spectroscopy with aids of density functional theory (DFT) calculations. The HQ monomer did not show any photo-reactivity at 350 nm but was photolyzed at 300 nm. The HQ–$(water)_n$ complex was found to be chemically transformed into p-benzoquinone (BQ)–$(water)_n$ with the 350 nm irradiation. The experimental threshold wavelength is almost comparable to the S_1–S_0 transition energy of HQ–$(water)_2$ estimated by a time-dependent DFT calculation. The observation indicates that two water molecules make electron-donated hydrogen-bonds with HQ and assist the photooxidation of HQ to BQ.

© 2011 Elsevier B.V. All rights reserved.

1. Introduction

Scheme 1 represents well-known reversible redox reactions, which chemically interconvert 1,4-hydroquinone (HQ), semiquinone radical, and p-benzoquinone (BQ). The reaction system serves as one prototype model for biological electron transfers working in photonic synthesis and respiration [1]. The reaction mechanisms in solutions have been studied with the thermodynamic characterization. The redox reactions are also induced by changing the pH value as well as by radiolysis or photolysis [2–4]. The intermediate semiquinone radical having a characteristic ring structure between aromatic HQ and non-aromatic quinonoid rings has attracted molecular scientists, and the step-wised redox reactions have been investigated in solutions using several spectroscopic experiments and theoretical calculations [5–15]. For example, Beck and Brus reported the production of semiquinone radical by photo-reducing BQ in aqua [14,15] or photo-oxidizing HQ in aqua [15]. The photo-reduction process has been proposed to occur through hydrogen abstraction by triplet BQ, while the hydrogen atom elimination is responsible for the oxidation of HQ. Although the photoinduced hydrogen-atom elimination seems to occur easily by the UV photolysis of HQ, the photoreaction has not been observed for gaseous HQ and therefore the semiquinone radical has not been detected in the gas phase up to date. Then, the difference between the photochemical reaction mechanisms in the gas and liquid phases indicates that HQ requires any solvated molecules for the photooxidation. In contrast to Scheme 1, the similar photoinduced step-wised oxidation process (Scheme 2) was observed in a low-temperature matrix [16]. "Scheme 1" becomes "Scheme 2" by replacing O-atoms by the isoelectronic NH radicals.

In the present study, we have performed the photolysis of HQ monomer in a low-temperature Ne matrix but could not identify any photoproduct assigned to semiquinone radical or BQ. The photochemistry of HQ in the cryogenic inert gas matrix was found to be different from the photo-oxidation process reported for HQ in aqueous solution, which may imply that the photo-oxidation of HQ needs some assistance such as hydration. The HQ–$(water)_n$ complex was found to be chemically transformed into p-benzoquinone (BQ)–$(water)_n$ with the 350 nm irradiation. We then studied the photochemistry of HQ–$(water)_n$ complexes as fundamental compositional units of aqueous HQ, and we could detect aqueous BQ as the photoproduct. The reaction mechanisms are discussed on the basis of the observation.

2. Experimental and calculation methods

A small amount of 1,4-hydroquinone or p-benzoquinone (Tokyo Chemical Industry) was placed in a stainless steel pipe nozzle equipped with a heating system. The HQ solid sample was heated at about 330 K, and the HQ vapor was mixed with carrier gas of pure Ne or Ne containing water. The BQ solid sample was evaporated at room temperature and mixed with carrier gas. The flow rate of the carrier gas was adjusted so to enable us to record the IR

* Corresponding authors. Tel.: +81 3 5734 2224; fax: +81 3 5734 2231.
E-mail addresses: akai.n.ab@m.titech.ac.jp (N. Akai), kshibuya@chem.titech.ac.jp (K. Shibuya).

1010-6030/$ – see front matter © 2011 Elsevier B.V. All rights reserved.
doi:10.1016/j.jphotochem.2011.08.016

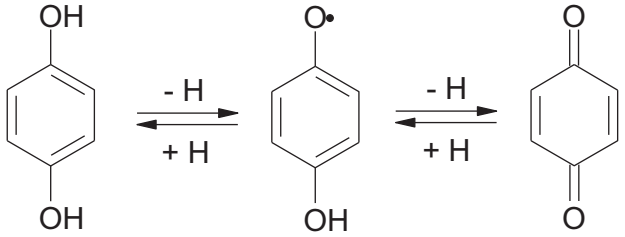

Scheme 1. Reversible redox reactions of 1,4-hydroquinone (HQ)/semiquinone radical/p-benzoquinone (BQ) systems.

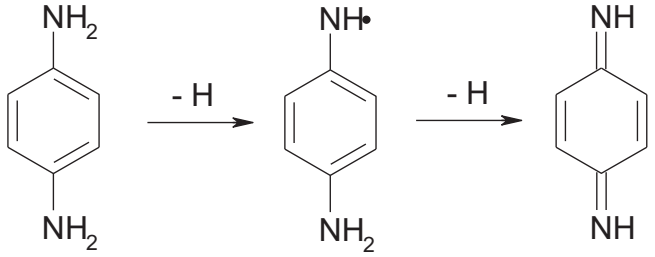

Scheme 2. Photoinduced one-way oxidation of 1,4-diaminobenzene/4-aminoanilino radical/2,5-cyclohexadiene-1,4-diimine systems.

spectra of isolated samples. The gas mixtures were expanded into a vacuum chamber through a stainless steel pipe and deposited on a CsI plate cooled by a closed-cycle helium refrigerator (Iwatani, Cryomini) at ca. 6 K. A combination of the UV radiation from a xenon lamp (Asahi Spectra, Max-302uv) with appropriate short-wavelength cut-off filters was used as a light source for photolysis.

Infrared spectra of the matrix isolated samples were measured with an FTIR spectrophotometer (Jeol, SPX 200ST). The spectral resolution was 0.5 cm^{-1} and the accumulation number was 100. Other experimental details were reported elsewhere [17].

Density functional theory (DFT) calculations were performed using the Gaussian 09 program with the 6-31++G** basis set [18]. The hybrid density functional at B3LYP [19,20] was used to optimize geometrical structures and to calculate their vibrational frequencies. The time-dependent DFT (TD-DFT) calculation was used to estimate vertical transition energies.

3. Results and discussion

3.1. Structures of hydroquinone–water complexes

The geometrical structures of HQ monomer and its water-complexes have been studied by laser spectroscopy with quantum chemical calculations [21–26]. We recalculated the optimized structures of HQ–$(water)_n$ complexes at the B3LYP/6-31++G** level. The resultant structures of the monomer and complexes, HQ–$(water)_{1,2}$, are shown in Fig. 1, and their relative energies with the wavelengths corresponding to the S_1–S_0 vertical transitions are summarized in Table 1. We use "a combination of alphabets" to specify HQ–water complex by (1) an OH-conformation within HQ (trans-form abbreviated as "t" or cis-form as "c") and (2) a type of HQ hydrogen-bonded with water (proton-donating type abbreviated as "D" or proton-accepting type as "A").

According to the B3LYP/6-31++G** level calculation [27], the energy difference of HQ–$(water)_1$ complexes comes from different hydrogen-bond structures of "D" and "A". It is recognized in Table 1 that the "Dt" structure is more stable by 11 kJ mol^{-1} than "At" though the difference between "Dt" and "Dc" is less than 1 kJ mol^{-1}. As illustrated in Fig. 1b, the hydrogen-bond lengths between HQ and water are estimated at 1.87 Å for "Dt"/"Dc", which are shorter by ~0.1 Å than 1.97 Å for "At"/"Ac". The OH bond lengths within HQ are 0.98 Å for "Dt"/"Dc", which are a little longer than 0.97 Å for "At"/"Ac" or HQ monomer. Our DFT calculation reproduces essentially the same HQ–$(water)_1$ geometry as reported one [23]. It is noticed that more stable "Dt"/"Dc" structures have much smaller S_1–S_0 vertical energies. Those vertical transition energies of "Dt"/"Dc" are smaller by ~7500 cm^{-1} than that of HQ monomer, though the corresponding transition energies are essentially the same for "At"/"Ac" or HQ monomer. Table 1 lists the wavelengths corresponding to the S_1–S_0 transition to be 331–333 nm for "Dt"/"Dc", which is definitely longer than 267–268 nm for "At"/"Ac". The red-shifted electronic absorption expected for the complexes of "Dt"/"Dc" structures are supposed to be weak judging from a fact that the large energy shifts have not been observed in the gas phase [23,26].

Table 1
Relative energies and S_1–S_0 transition wavelengths of HQ–$(water)_n$ (n = 0–2) estimated at the B3LYP/6-31++G** level.

	Relative energies/kJ mol^{-1} (numbers of hydrogen bond)	Wavelengths corresponding to the S_1–S_0 transition/nm
HQ		
Trans	0	265
Cis	0.6	270
HQ–$(water)_1$		
"Dt"	0 (1)	331
"Dc"	0.4 (1)	333
"At"	11.1 (1)	267
"Ac"	12.2 (1)	268
HQ–$(water)_2$		
"ADc"	0 (3)	281
"ADt"	0.2 (3)	281
"DtD"	15.1 (2)	357
"DcD"	15.4 (2)	358
"AtD"	22.4 (2)	315
"AcD"	22.9 (2)	316
"AtA"	34.7 (2)	261
"AcA"	37.1 (2)	262

Eight stable structures for HQ–$(water)_2$ are shown in Fig. 1c, and the relative energies are listed in Table 1, together with the wavelengths corresponding to the S_1–S_0 vertical transitions. The most stable "ADt"/"ADc" structure is of a ring-type with three hydrogen bonds. The second stable "DtD"/"DcD" structures have two hydrogen bonds so that HQ acts as a double proton-donor or a double electron acceptor (Fig. 1c). The S_1–S_0 transition energies of "DtD"/"DcD" are red-shifted by ~9500 cm^{-1} from the S_1–S_0 gap of HQ monomer. The electronic absorption bands of "DtD"/"DcD" are then estimated to appear at 357 and 358 nm, respectively (Table 1). It suggests that only the red-shifted absorption bands of "DtD"/"DcD" are separated from those of the other six structures of HQ–$(water)_2$.

Fig. 2 shows HOMOs and LUMOs of HQ–$(water)_n$ (n = 0, 1, and 2). Each molecular orbital of the S_1 state is characterized by an admixture of the respective LUMO and other molecular orbitals. The large shift in the S_1–S_0 transition energy may be explained by characteristics of LUMO. It is noticed that the LUMOs of complexes including "D" water are localized on the water molecules, while the LUMOs of "At" and "AtA" complexes are essentially the same as the π^* orbital of HQ monomer. This computational result indicates that charge transfer state characters are generated for the electronically excited S_1 states of the water-complexes, though the details are not well understood yet. Although the HOMO–LUMO transition are expected to be forbidden, the electronic transitions may be induced by perturbation as described later. The π–π^* transition energies of "Dt", "Dc", "DtD" and "DcD" correspond to the wavelengths of 273, 273, 276 and 276 nm,

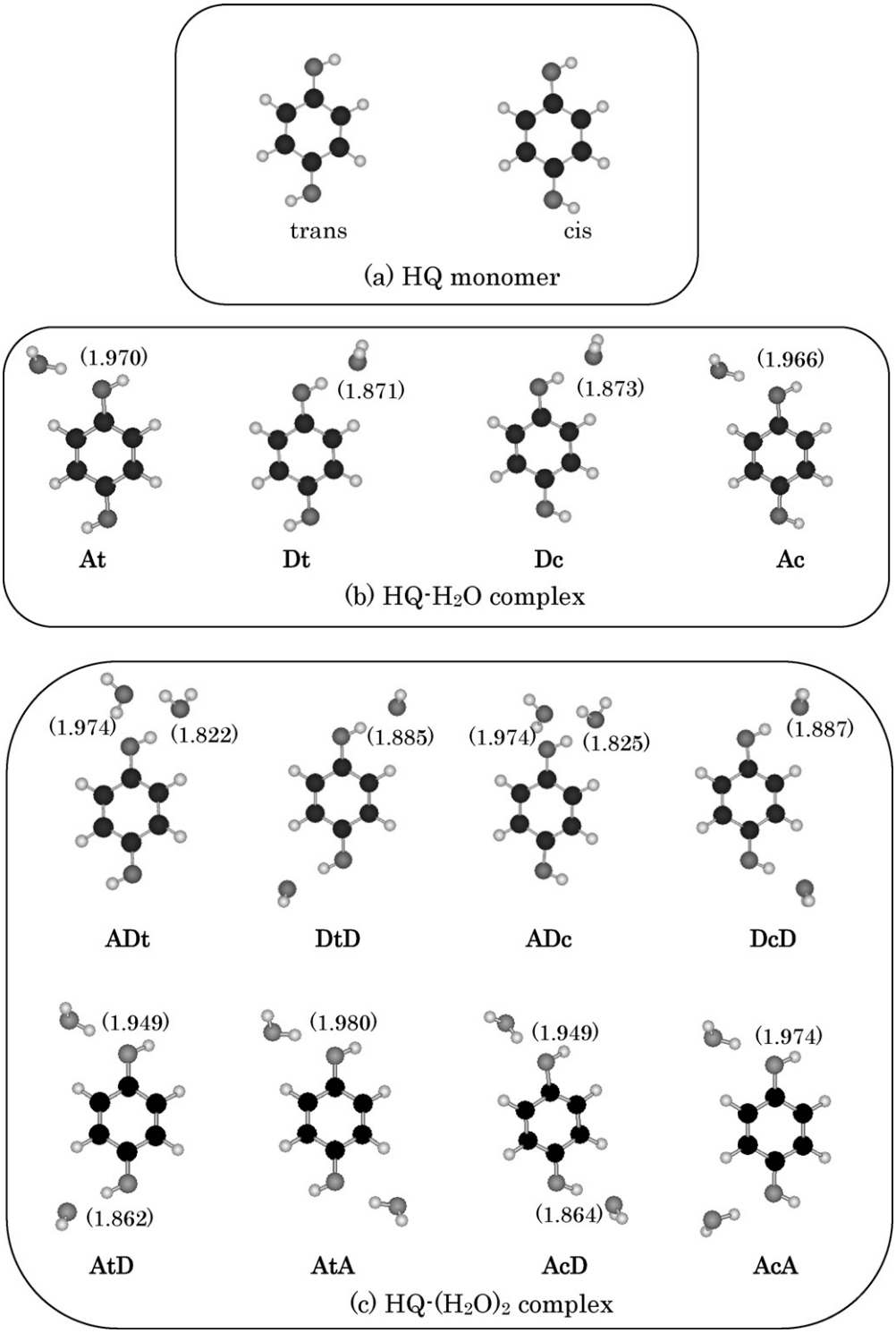

Fig. 1. Structures of HQ–(water)$_n$ (n = 0, 1, 2) complexes. The numbers in parentheses are hydrogen bond length (in Å) estimated at the B3LYP/6-31++G** level. (a) HQ monomer, (b) HQ–H_2O complex and (c) HQ–$(H_2O)_2$ complex.

respectively, which are comparable with 265–270 nm of HQ monomer. The S_1–S_0 transitions of HQ with "A"-waters are characterized by the π–π^* transition and their transition wavelengths also are close to that of HQ monomer.

The complex structures of HQ–(water)$_n$ ($n \geq 3$) will contain essentially one of the eight HQ–(water)$_2$ structures shown in Fig. 1c. The transition energies of such larger complexes are expected to reflect the hydrogen bond types of HQ–(water)$_2$. It means that the S_1–S_0 transition energy of larger complexes is similar with that for one of eight water–HQ–water structures. In fact, the S_1–S_0 transitions of HQ with "D"-waters are of the HQ-to-water charge transfer type and are located at largely red-shifted wavelengths. The HQ–(water)$_2$ core structure might be important in the photochemistry of larger water-complexes of HQ.

One must be careful to use the relative energies listed in Table 1. The relative energy is mainly controlled by two factors, (1) the

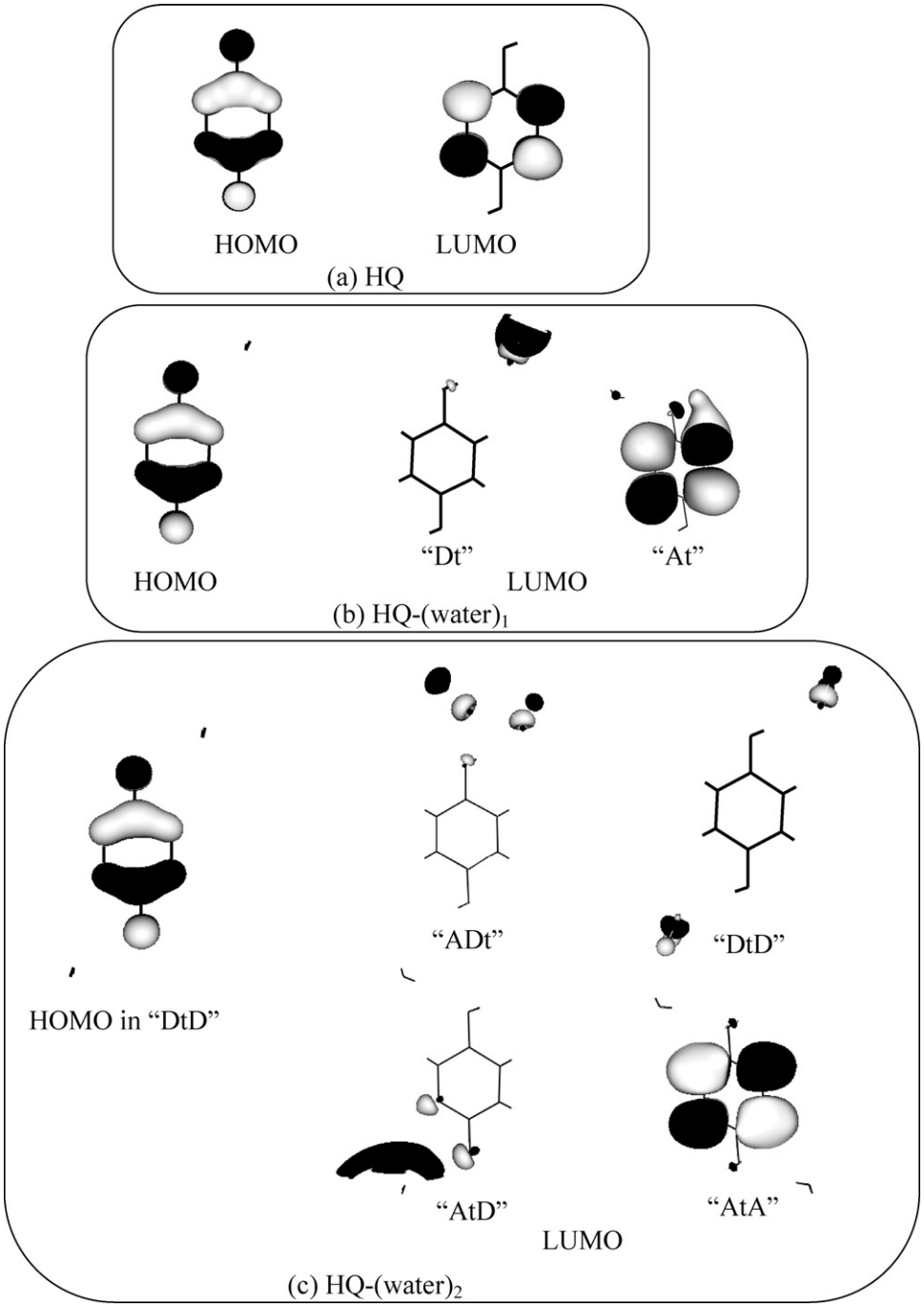

Fig. 2. Graphical picture of molecular orbitals. HOMO and LUMO are illustrated for (a) HQ monomer in the trans-form, (b) HQ–(water)$_1$, and (c) HQ–(water)$_2$. Black and white colored orbitals correspond to positive and negative phases of the wavefunction.

number of hydrogen bonds and (2) "A"/"D" structures. Among eight HQ–(water)$_2$ complexes, two "ADc" and "ADt" structures contain three hydrogen bonds, while the other six structures have only two hydrogen bonds. This is the reason why the "ADc" and "ADt" structures are listed as the lowest among the HQ–(water)$_2$ complexes. More importantly, the core structure will be essentially one of the six structures ("DtD", "DcD", "AtD", "AcD", "AtA", and "AcA"), when HQ–(water)$_n$ ($n \geq 3$) complex becomes larger.

3.2. IR spectra of hydroquinone monomer and the water-complex

Fig. 3 shows the matrix isolation IR spectra of HQ monomer and HQ–water complexes in solid Ne. The trans- and cis-conformers of HQ were spectroscopically separated in argon and xenon matrices upon UV irradiation [27]. But in the present study using a cryogenic neon matrix, we could not identify the two isomers and then the trans/cis isomerization was not observed. The HQ monomer has some intense sharp IR bands at 759 (C–O stretching), 1250 (C–H in-plane bending) and 1520 (C–H in-plane bending) cm^{-1} as shown in Fig. 3a. These HQ bands are close to the reported bands measured in different matrixes within 2 cm^{-1} [27]. The sharp and intense C–O–H bending band at 1159 cm^{-1} was reported for trans-HQ in an Ar matrix [27], but the corresponding 1165 cm^{-1} band in a Ne matrix was broad and accompanied by several sidebands at the blue-side.

With increasing water concentration, the IR bandwidths of HQ become broad but any new band of HQ–water complexes does

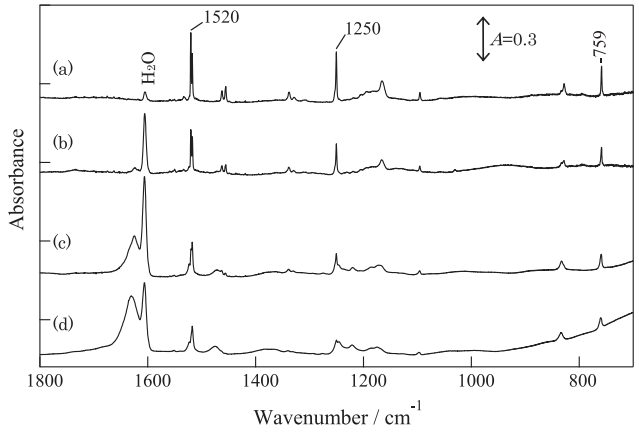

Fig. 3. Infrared spectra of HQ monomer and HQ–(water)$_n$ complexes isolated in a neon matrix. The water/Ne dilution ratios were (a) 0%, (b) 1%, (c) 2% and (d) 3%. A trace of water impurity was recognized in (a).

not appear as shown in Fig. 3b–d. The 1600 cm^{-1} band is mainly due to the bending mode of H_2O, which is accompanied by the 1630 cm^{-1} satellite band due to $(H_2O)_n$. The water multimer bands become stronger with increasing the water/Ne dilution ratio. Possibly, the complex bands due to HQ–(water)$_n$ are buried in the broad 1600 and 1630 cm^{-1} bands. It will be expected greater contribution of HQ–(water)$_n$ complexes with increasing the water concentration. In fact, the spectral shape of Fig. 3d becomes broader than those of Fig. 3a, which will be confirmed by the negative signals (Figs. 4 and 5) observed in the photolysis experiments described later. In the matrix made by the water/Ne ratio of 3%, larger complexes of HQ–(water)$_n$ ($n \geq 3$) generated are expected to contain HQ–$(H_2O)_2$ core structures illustrated in Fig. 1c.

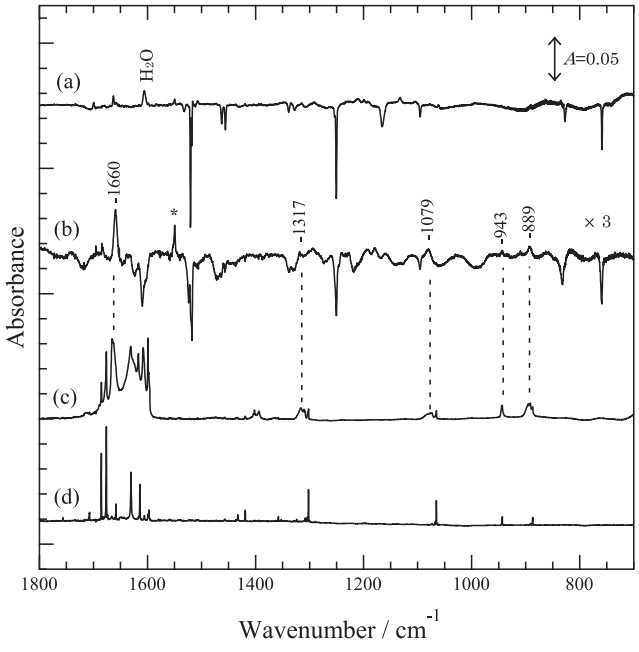

Fig. 4. Infrared spectra relevant to UV-light induced reactions of HQ monomer and HQ–(water)$_n$ complexes. Difference spectra of HQ in a pure Ne matrix upon the 300 nm irradiation for 15 min (a), and HQ in a 3% water/Ne matrix upon the 350 nm irradiation for 80 min (b). The negative and positive signals originate with reactant(s) and product(s), respectively. Two reference IR spectra of BQ were recorded in a 3% water/Ne matrix (c) and in a pure Ne matrix (d). The band marked with asterisk in (b) is due to unidentified photoproducts.

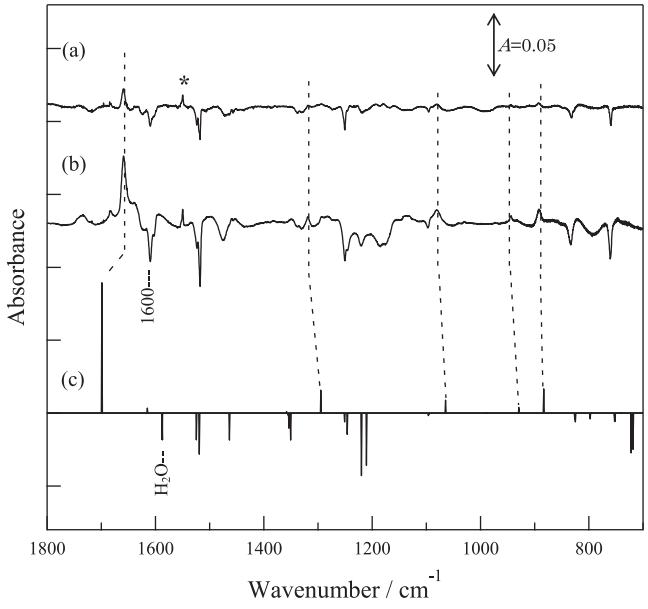

Fig. 5. Comparison of experimental and simulated infrared difference spectra relevant to the UV-light induced reactions of HQ monomer and HQ–(water)$_n$ complexes. Two difference spectra of HQ in a 3% water/Ne matrix are shown: The spectrum (a) is the same as Fig. 3b, and the spectrum (b) was obtained by the 325 nm irradiation for 30 min. The simulated IR spectra (c) are composed of the positive bars of BQ product and the negative bars of HQ–(water)$_2$ reactants in the "DtD" and "DcD", where all calculated wavenumbers are adjusted by a scaling factor of 0.98. The band marked with asterisk is assigned to unidentified photoproducts.

3.3. UV light induced reactions of HQ monomer and HQ–(water)$_n$ complexes

Fig. 4a and b shows difference spectra recorded upon the UV-light irradiation of HQ monomer and HQ–(water)$_n$ complexes, respectively, isolated in Ne matrixes. HQ monomer did not show any photochemical change upon the 350 nm irradiation, but photodecomposed at 300 nm as shown in Fig. 4a. The HQ monomer was photolyzed with the production of unknown species corresponding to weak positive bands (1699, 1663, 1550, 1132 cm^{-1} etc.). The positive bands were assigned to neither BQ nor semiquinone radical, which were reported upon the 266 nm light irradiation of HQ in aqueous solution [15]. It turns out that BQ or semiquinone radical is not produced in the UV photolysis of HQ monomer. Naturally, any photo-product was not generated in the UV photolysis of pure (water)$_n$ complexes, which did not contain HQ.

Fig. 4b indicates that HQ–(water)$_n$ complex is transformed into some product(s) upon the 350 nm irradiation. The positive bands at 1660, 1550, 1317, 1079, 943 and 889 cm^{-1} are assigned to the photoreaction product(s). The intense 1660 cm^{-1} band is definitely assigned to a quinonoid C=O stretching mode, which may imply that the product is BQ. However, the positive bands of Fig. 4b are slightly different from those of BQ measured in an Ar matrix [28], and then we measured the IR spectra of BQ and BQ–(water)$_n$ in a Ne matrix. Fig. 4c and d shows the matrix isolation IR spectra of BQ in 3% water/Ne and pure Ne matrices, respectively. Almost all bands in Fig. 4c would be identified as BQ–(water)$_n$ and (water)$_n$ complexes. Except for the 1550 cm^{-1} band, the positive product bands observed in Fig. 4b correspond to the BQ–(water)$_n$ bands. It is then concluded that BQ–(water)$_n$ are produced upon the 350 nm irradiation of HQ–(water)$_n$.

The negative bands in Fig. 4b accord with those of the HQ–(water)$_n$ complexes, which are shown in Fig. 3. The strong bands around 1600 cm^{-1} assigned as the water bending mode of

HQ–(water)$_n$ complexes. HQ–(water)$_n$ complexes are surely the photo-reactant to generate the HQ–(water)$_n$ product. As described earlier in this paper, HQ–(water)$_2$ isomers of "DtD" and "DcD" structures are predicted to absorb longer-wavelength lights around 360 nm (Table 1), which supports our experimental observation that the photo-reaction takes place at wavelengths around 350 nm. The HQ chromophore of additionally hydrated HQ–(water)$_n$ ($n \geq 3$) will have essentially the same chromophore as HQ–(water)$_2$ in the "DtD" and "DcD" structures. Then, HQ–(water)$_n$ ($n \geq 3$) complexes containing the HQ–(water)$_2$ core in the "DtD" and "DcD" structures also will absorb UV light near 350 nm.

In Fig. 5, we compare two experimental difference spectra (a and b) with the simulated spectrum (c). Two difference spectra of HQ in a 3% water/Ne matrix were obtained upon the irradiation at (a) 350 nm and (b) 325 nm. The 325 nm irradiation results in the spectral measurement easily to identify the reactant and product species of the present interest. The spectral patterns of the observed difference spectra shown in Fig. 5a and b are similar with each other. Fig. 5c shows the simulated IR spectra composed of the positive bars due to BQ product and the negative bars due to HQ–(water)$_2$ reactant as "DtD" and "DcD". The agreement between experiment and simulation seems reasonably good. It is important that the H_2O bending mode of the complexes calculated around 1588 cm^{-1} reproduces the 1600 cm^{-1} band in the experimental spectrum. The correspondence relation supports that the HQ–(water)$_n$ is the photo-reactants responsible for the BQ–(water)$_n$ products. We conclude that the 1550 cm^{-1} band is not due to BQ–(water)$_n$, because (1) the IR intensity patterns are different for different photolysis wavelengths (Fig. 5a for 350 nm and Fig. 5b for 325 nm) and (2) the 1550 cm^{-1} band does not appear in the simulated spectrum (Fig. 5c).

We attempted to detect semiquinone radical and semiquinone radical anion expected as the photoproducts by hydrogen-atom elimination and proton transfer reactions. But we could not identify such species. Radical species produced by hydrogen-atom elimination reaction is known to be consumed through the recombination with hydrogen-atom diffusing and to recover the parent molecules in solid Ne [29,30]. But we could not find any positive or negative peak in the dark or even after annealing. Such an H-elimination process does not seem to occur in the present photolytic system.

3.4. On the UV absorption of HQ–(water)$_n$ complex

It turns out that the HQ to BQ photooxidation does not occur as the unimolecular primary process in the UV photolysis but proceeds as water-mediated process through the hydrogen-bonded complex formation with HQ. The S_0 states of the HQ monomer and the water-complexes are mainly characterized by the π orbitals on the aromatic ring as shown in Fig. 2. On the other hand, the LUMOs of the water-complexes are localized on the water moieties though the LUMO of HQ is the π^* orbital on the ring. As described previously, the S_1–S_0 transition energies for the "Dt" and "DtD" complexes are apparently lower than the corresponding energies of HQ monomer or other water-complexes such as "At" and "AtA" (Table 1). The S_1 states of "Dt" and "DtD" are mainly characterized by the intermolecular charge-transfer states generated by promoting an electron from the HOMO on the HQ ring to the LUMO localized on water. Although the S_1–S_0 transitions are forbidden in nature, it would be slightly induced by perturbations from matrix medium and/or the complex vibration. The π–π^* transitions of "Dt" and "DtD" are estimated to be 273 and 276 nm, which are similar with those of HQ monomers. It indicates that the π–π^* transitions of the complexes do not occur upon the irradiation light at 350 nm.

We expected to detect semiquinone radical and BQ from HQ or HQ–(water)$_n$ complexes upon the UV-light irradiation before we started a series of experiments. But any band assigned as semiquinone radical was not recognized among the photoproducts under various water/Ne dilution conditions. The B3LYP calculation suggests that a molecular system of semiquinone radical–H–H_2O, even if it is formed from the UV-irradiation, is unstable and returns to the stable HQ–water pair through hydrogen atom backward transfer. In the present experiments, we observed the production of BQ as the photoproduct but could not identify the intermediate semiquinone radical shown in Scheme 1. The HQ to BQ photooxidation seems to occur through a reaction mechanism with transferring two H-atoms from one HQ to two H-bonded water molecules. We tentatively conclude that the photooxidation occurs by a two H-atom dissociation process of water –HQ–water.

4. Summary

The UV photoreaction product from HQ–(water)$_n$ isolated in a Ne matrix was investigated by IR spectroscopy with aids of DFT calculations. The HQ–(water)$_n$ complex was found to be chemically transformed into BQ–(water)$_n$ with the 350 nm irradiation, while HQ monomer did not yield BQ upon the UV light irradiation. The TD-DFT calculation suggests that the photoreaction originates with the water-complex of HQ–(water)$_n$. The S_1–S_0 transition wavelength of HQ–(water)$_2$ complexes in the "DtD" and "DcD" structures, is calculated to be largely red-shifted from that of HQ monomer, which is satisfactorily consistent with the experimental results for the photoreaction from HQ–(water)$_n$ to BQ.

Acknowledgments

This work was supported in part by Grant-in-Aid for Young Scientists (B) (No. 22750010) and Scientific Research on Priority Areas (No. 22018005) from the Ministry of Education, Culture, Sports, Science and Technology, Japan.

References

[1] R. Foster, M.I. Forman, The Chemistry of Quinoid Compounds, Wiley, New York, 1974.
[2] P.D. Astudillo, J. Tiburcio, F.J. Gonzalez, J. Electroanal. Chem. 604 (2007) 57.
[3] C. Nishizawa, K. Takeshita, J. Ueda, I. Nakanishi, K. Suzuki, T. Ozawa, Free Radic. Res. 40 (2006) 233.
[4] O. Brede, S. Kapoor, T. Mukherjee, R. Hermann, S. Naumov, Phys. Chem. Chem. Phys. 4 (2002) 5096.
[5] R. Beck, J.W. Nibler, J. Chem. Educ. 66 (1989) 263.
[6] M. Jäger, J.R. Norris Jr., J. Magn. Reson. 150 (2001) 26.
[7] M. Nonella, J. Phys. Chem. B 101 (1997) 1235.
[8] A.M. Mebel, M.C. Lin, J. Am. Chem. Soc. 116 (1994) 9577.
[9] P. Mohandas, S. Umapathy, J. Phys. Chem. A 101 (1997) 4449.
[10] J. Cheng, M. Sulpizi, M. Sprik, J. Chem. Phys. 131 (2009) 154504.
[11] G.N.R. Tripathi, R.H. Schuler, J. Phys. Chem. 91 (1987) 5881.
[12] G.N.R. Tripathi, J. Am. Chem. Soc. 120 (1998) 5134.
[13] X. Zhao, H. Imahori, C.-G. Zhan, Y. Sakata, S. Iwata, T. Kitagawa, J. Phys. Chem. A 101 (1997) 622.
[14] S.M. Beck, L.E. Brus, J. Am. Chem. Soc. 104 (1982) 1103.
[15] S.M. Beck, L.E. Brus, J. Am. Chem. Soc. 104 (1982) 4789.
[16] N. Akai, S. Kudoh, M. Nakata, J. Phys. Chem. A 107 (2003) 6725.
[17] M. Tsuge, K. Tsuji, A. Kawai, K. Shibuya, J. Phys. Chem. A 111 (2007) 3540.
[18] M.J. Frisch, G.W. Trucks, H.B. Schlegel, G.E. Scuseria, M.A. Robb, J.R. Cheeseman, G. Scalmani, V. Barone, B. Mennucci, G.A. Petersson, H. Nakatsuji, M. Caricato, X. Li, H.P. Hratchian, A.F. Izmaylov, J. Bloino, G. Zheng, J.L. Sonnenberg, M. Hada, M. Ehara, K. Toyota, R. Fukuda, J. Hasegawa, M. Ishida, T. Nakajima, Y. Honda, O. Kitao, H. Nakai, T. Vreven, J.A. Montgomery Jr., J.E. Peralta, F. Ogliaro, M. Bearpark, J.J. Heyd, E. Brothers, K.N. Kudin, V.N. Staroverov, R. Kobayashi, J. Normand, K. Raghavachari, A. Rendell, J.C. Burant, S.S. Iyengar, J. Tomasi, M. Cossi, N. Rega, J.M. Millam, M. Klene, J.E. Knox, J.B. Cross, V. Bakken, C. Adamo, J. Jaramillo, R. Gomperts, R.E. Stratmann, O. Yazyev, A.J. Austin, R. Cammi, C. Pomelli, J.W. Ochterski, R.L. Martin, K. Morokuma, V.G. Zakrzewski, G.A. Voth, P. Salvador, J.J. Dannenberg, S. Dapprich, A.D. Daniels, Ö. Farkas, J.B. Foresman, J.V. Ortiz, J. Cioslowski, D.J. Fox, Gaussian 09, Revision A.1, Gaussian, Inc., Wallingford, CT, 2009.

[19] A.D. Becke, J. Chem. Phys. 98 (1993) 5648.
[20] C. Lee, W. Yang, R.G. Parr, Phys. Rev. B 37 (1988) 785.
[21] T.M. Dunn, R. Tembreull, D.M. Lubman, Chem. Phys. Lett. 121 (1985) 453.
[22] G.N. Patwari, S. Doraiswamy, S. Wategaonkar, Chem. Phys. Lett. 289 (1998) 8.
[23] P.S. Meenakshi, N. Biswas, S. Wategaonkar, Phys. Chem. Chem. Phys. 5 (2003) 294.
[24] N. Biswas, S. Chakraborty, S. Wategaonkar, J. Phys. Chem. A 108 (2004) 9074.
[25] K. Hattori, S. Ishiuchi, M. Fujii, D.L. Howard, H.G. Kjaergaard, J. Phys. Chem. A 111 (2007) 6028.
[26] S. Chakraborty, P. Misra, S. Wategaonkar, J. Chem. Phys. 127 (2007) 124317.
[27] N. Akai, S. Kudoh, M. Takayanagi, M. Nakata, Chem. Phys. Lett. 356 (2002) 133.
[28] A.M. Plokhotnichenko, E.D. Radchenko, S.G. Stepanian, L. Adamowicz, J. Phys. Chem. A 103 (1999) 11052.
[29] N. Akai, H. Yoshida, K. Ohno, M. Aida, Chem. Phys. Lett. 403 (2005) 390.
[30] K. Tsuji, K. Shibuya, J. Phys. Chem. A 113 (2009) 9945.